Journal of Power Sources 228 (2013) 7–13

Contents lists available at SciVerse ScienceDirect

Journal of Power Sources

journal homepage: www.elsevier.com/locate/jpowsour

Walnut-like vanadium oxide film with high rate performance as a cathode material for rechargeable lithium batteries

Yi Sun [a,b], Linchao Zhang [a], Suqing Wang [a], Ingo Lieberwirth [b], Yan Yu [a], ChunHua Chen [a,*]

[a] CAS Key Laboratory of Materials for Energy Conversion, Department of Materials Science and Engineering, University of Science and Technology of China, Hefei, Anhui 230026, China
[b] Max Planck Institute for Polymer Research, Mainz 55128, Germany

HIGHLIGHTS

- ► Fabrication of a nanoporous vanadium oxide film by using a suspension instead of usual solution as ESD precursor.
- ► The use electron energy loss spectrum (EELS) technique to determine vanadium valence in the nanocomposite film.
- ► Vanadium oxide film shows excellent electrochemical properties.

ARTICLE INFO

Article history:
Received 27 August 2012
Received in revised form
23 November 2012
Accepted 24 November 2012
Available online 29 November 2012

Keywords:
Electrostatic spray deposition
Film
Nanostructure
Vanadium oxide
Lithium-ion battery

ABSTRACT

Vanadium oxide films composed of porous walnut-like particles are fabricated by electrostatic spray deposition (ESD) with an oil-bathed suspension precursor. The micron-sized particles are constructed from vanadium oxide nanocrystals of size around 50–100 nm and the valence of vanadium is determined by electron energy loss spectroscopy (EELS). As a cathode material for rechargeable lithium batteries, it exhibits stable reversible specific capacity and ultra-high rate capability. It delivers a specific discharge capacity of 254 mAh g^{-1} in first cycle, and still maintains 200 mAh g^{-1} after 100 cycles in the voltage range of 2.1–4.0 V. When the cell is cycled between 2.5 and 4.0 V, its discharge capacity reaches 103 mAh g^{-1} at 50 C and reserves 85 mAh g^{-1} at 10 C even at −10 °C.

1. Introduction

Rechargeable lithium ion batteries, which have been widely applied in portable devices and power tools, play an important role in modern society [1]. Nevertheless, it is urgent to improve the rate capability and energy density in order to satisfy the needs of the applications of electric vehicles (EV), hybrid electric vehicles (HEV) and large-scale energy storage systems. Because the rate of mass transport is substantially decreased at low temperatures below room temperature, it should be important to pay attention to the low-temperature performance of Li-ion batteries for the operation of EV or HEV in winter time. Layer-structured vanadium oxides, such as V_2O_5 and VO_2, due to their high theoretical capacity (294 mAh g^{-1} for $Li_2V_2O_5$ and 161 mAh g^{-1} for $Li_{0.5}VO_2$), low cost, are considered to be candidates of cathode materials for lithium ion batteries [2–4].

Nevertheless, the low diffusion coefficient of lithium ions ($\sim 10^{-12}$ cm^2 s^{-1} for V_2O_5) [5] and the poor electronic conductivity (10^{-2} to 10^{-3} S cm^{-1} for V_2O_5) hinder their practical applications [6]. To improve the electrochemical performance, various nanostructures of vanadium oxides, such as nanorods, nanoparticles, nanotubes and mesoporous structures have been synthesized by different methods (e.g., hydrothermal method, electrodeposition, and sol–gel process) [7–10]. Moreover, the electrodes composed of nanoparticles exhibit improved low-temperature performance [11,12]. Here, we report that a nanostructured vanadium oxide film with mixed +4/+5 valence states is fabricated by electrostatic spray deposition (ESD) technique with a pre-prepared stable suspension instead of a commonly clear solution as the ESD precursor. Compared with other film fabrication methods such ultrasonic or pneumatic spraying, screen printing and doctor-blade tape casting, the ESD method has advantages of high deposition rate, easy control of the film morphology and the need of only small quantity

* Corresponding author. Tel.: +86 551 3606971; fax: +86 551 3601592.
E-mail address: cchchen@ustc.edu.cn (C. Chen).

0378-7753/$ – see front matter © 2012 Elsevier B.V. All rights reserved.
http://dx.doi.org/10.1016/j.jpowsour.2012.11.095

of precursors. In our previous work, a series of metal oxide films as anode material have been prepared by this facile method [13,14], but few cathode films have been prepared [15]. This binder-free vanadium oxide film exhibits high and stable reversible specific capacity and excellent rate capability as a cathode material.

2. Experimental

Firstly, 0.01 M NH_4VO_3 was dissolved into the solvent which contained 1.0 ml H_2O, 19.5 ml ethylene glycol (EG) and 19.5 ml 1,2-propanediol (1,2-Pr) at 80 °C and stirred for 1 h. Then, this light yellow solution was oil bathed at 170 °C for 3 h to obtain a precursor suspension. For structural analysis, the solid component of the suspension was also collected by centrifugation and washed with absolute ethanol for several times. Then film was deposited by the ESD technique for 3–4 h on a carbon plate substrate which was heated at 240 °C. The distance between the substrate and the needle was about 2–3 cm. The applied direct current voltage was 9–11 kV between the substrate and the needle, while the feed rate of the precursor suspension was 1.8 ml h^{-1} by a syringe pump. The suspension precursor was stable for around 4 h during intermittent stirring. After deposition, the mass of the film is about 2–3 mg and the coated area is 95 mm^2 on the round substrate ($\varnothing = 12$ mm). The deposition process was repeated for several times to obtain a few films. Then the films were annealed at 350 °C for 2.5 h in a muffle furnace to achieve a high degree of crystallization. The mass of vanadium oxide loading on each annealed film was about 1 mg.

The morphologies of the solid component from the suspension and the films were studied by scanning electron microscopy (SEM, JEOL-6390 LA) and transmission electron microscopy (TEM, Hitachi H-800). The crystal structures of the films were analyzed by x-ray diffraction (Rigaku TTR-III, Cu K_α radiation, $\lambda = 0.15418$ nm). The oxidation state of *V* in an annealed vanadium oxide film was characterized by electron energy loss (EEL) spectroscopy (Zeiss 912 microscope operated at 120 kV with an in-column omega energy filter).

The electrochemical properties of the films were measured using CR 2032 coin cells with the films as the working electrodes and Li foil as the counter electrode, while the electrolyte was 1 M $LiPF_6$ in ethylene carbonate/diethyl carbonate (1:1 *v*/*v*). The cells were assembled in an argon-filled glove box (MBRAUN LABMASTER 130) containing less than 1 ppm each of moisture and oxygen. Cyclic voltammetry (CV) measurements were performed on an electrochemical workstation (CHI 604B) with different scanning rates of 0.1–0.5 mV s^{-1} in the voltage range of 2.0–4.0 V or 2.5–4.0 V. After each CV run, the open circuit voltage of the cell was about 3.5 V. The cells were also cycled on a multi-channel battery cycler (NEWWARE BTS-610) in two voltage ranges, i.e. 2.1–4.0 V and 2.5–4.0 V, at room temperature, −10 and −20 °C, respectively.

3. Results and discussion

Fig. 1 exhibits the SEM and TEM images of the particles from the oil-bathed suspension. It can be seen that the particles from the suspension are roughly spherical with a diameter of about 1–2 μm (Fig. 1a). With a lager magnification, each particle is actually an agglomerate of many submicron primary particles and it is porous (Fig. 1b). The porous agglomerate structure is confirmed by its TEM image (Fig. 1c). Meanwhile, the XRD pattern of this powder exhibits a strong diffraction peak in the low-angle region (around 12°) (Fig. 1d), which is usually characteristic of a metal alkoxide [16–18]. Considering the precursors used and the probable reaction mechanism, its composition should be one kind of vanadium alkoxide.

After the ESD process and subsequent heat treatment, the obtained film consists of interconnecting walnut-like particles (Fig. 2a and b), which are more porous than those alkoxide particles obtained after the oil bath process (Fig. 1b). In fact, these walnut-like particles are composed of lots of small nanocrystals (about 50–100 nm) and nanopores (Fig. 2b). This porous structure is beneficial to achieve a large contact area between the electrolyte and such a vanadium-oxide electrode in a cell. The film is not very uniform in the direction of thickness with the thickness of the film is about 10–20 μm (Fig. 2c). Its overall porosity can be estimated as about 68% after considering the mass of the film and the density of V_2O_5. The films are scraped from the substrate for XRD analysis. Expect for the peak attributed to the graphitic carbon (JCPDS card no.89-

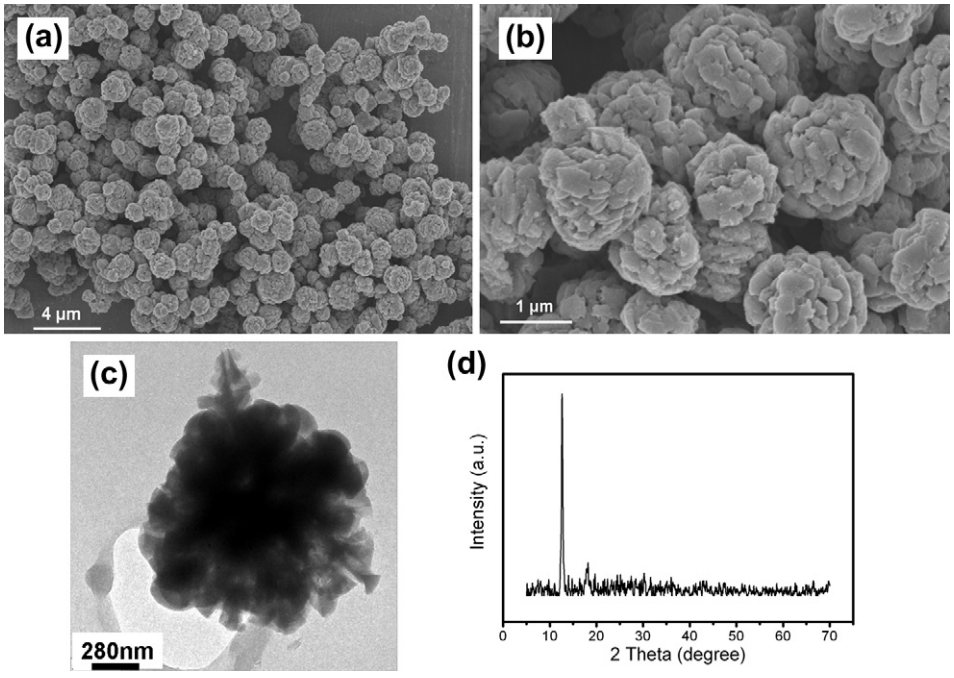

Fig. 1. (a and b) SEM and (c) TEM images of the solid component of the oil-bathed suspension; (d) XRD patterns of the powder.

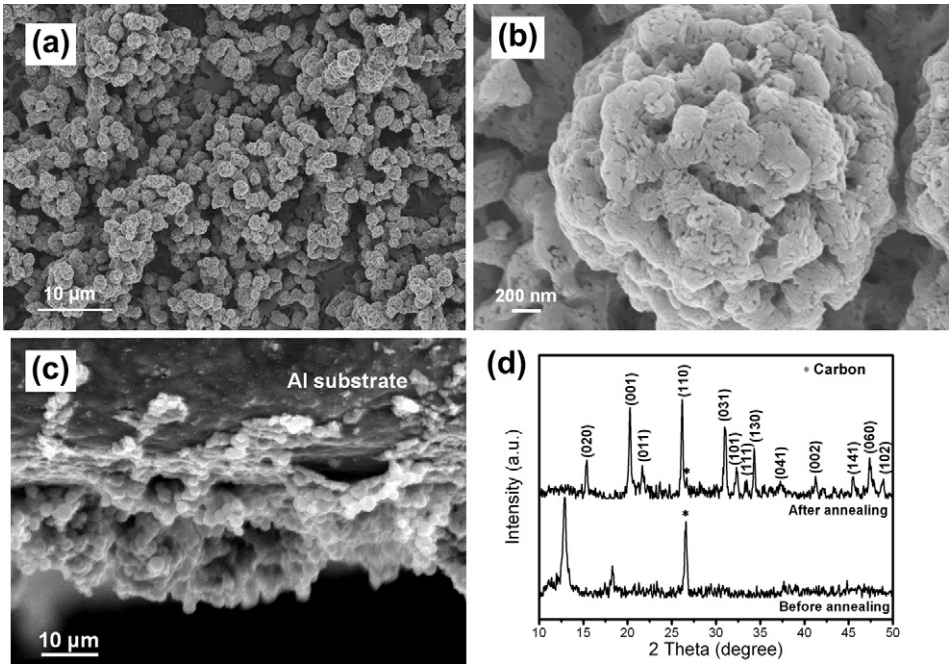

Fig. 2. (a and b) SEM and (c) cross section images of the annealed film on Al substrate; (d) XRD patterns of the as-deposited and annealed films scraped from the carbon substrate.

8487) from the scraped carbon substrate, the XRD pattern of the film before annealing is similar to that of the vanadium alkoxide (Fig. 1d), which can be stable at the low deposition temperature (240 °C) (Fig. 2d). After the 350 °C annealing in air, the film can be identified as V_2O_5 (JCPDS card no.85-0601).

The formation of V_2O_5 is also confirmed by the EEL analysis (Fig. 3). Two selected areas for the analysis are several interconnected nanocrystals at the inside of a secondary particle (region A, Fig. 3a) and the part close to the particle surface (region B, Fig. 3b). It can be seen from the spectra (Fig. 3c) that there are peaks from vanadium L_3 (corresponding to four $2p^{3/2} \rightarrow 3d^{3/2}3d^{5/2}$) and L_2 (corresponding to two $2p^{1/2} \rightarrow 3d^{3/2}$) edges in the energy range 515–529 eV, and the oxygen K edge at around 532.6 eV. The spectrum from region A exhibits two peaks at 520 (L_3) and 526.4 eV (L_2), respectively, featured by the V L-edge. Meanwhile, these two peaks shift to 519.1 and 525.4 eV in the spectrum of region B. The distance between the V–L_3 edge and the O–K peak (ΔE) is 12.6 and 13.5 eV for region A and region B, respectively. By comparing the energy positions of the white lines reported by Ding et al. [19] and the ΔE values reported by Gallasch et al. [20], the valences of vanadium in region A and region B can be determined as +5 and +4, respectively, indicating that some V^{5+} has been reduced into V^{4+} by the carbon substrate during the annealing process. The reduced region should be amorphous or poorly crystalline because no diffraction peaks of the V^{4+} composition is detected in the XRD pattern even if the film is scraped from the carbon substrate for the analysis (Fig. 2d).

The electrochemical properties of the vanadium oxide film electrode were investigated in coin-type half-cells in different voltage ranges. Fig. 4a shows the voltage profile of the vanadium oxide film electrode at 0.45 C (1 C = 294 mA g^{-1}) in the voltage range of 2.1–4.0 V. The first discharge and charge display typical plateaus at around 3.4, 3.2 and 2.2 V corresponding to the lithiations of ε, δ and γ phases of V_2O_5 in three steps [21,22]:

$$0.5Li^+ + 0.5e^- + V_2O_5 \leftarrow \rightarrow Li_{0.5}V_2O_5.$$

$$0.5Li^+ + 0.5e^- + Li_{0.5}V_2O_5 \leftarrow \rightarrow LiV_2O_5.$$

$$Li^+ + e^- + LiV_2O_5 \leftarrow \rightarrow Li_2V_2O_5.$$

However, compared with the typical V_2O_5 cathode, there are two small additional plateaus at around 2.85 and 2.5 V, which should be resulted from the active vanadium oxide with lower valence states of vanadium [23,24], that contains V^{4+}, as shown in the EEL spectrum (Fig. 3c). The electrochemical reaction steps can be can be written as following [19,23]:

$$0.1Li^+ + 0.1e^- + VO_2 \leftarrow \rightarrow Li_{0.1}VO_2$$

$$0.4Li^+ + 0.4e^- + Li_{0.1}VO_2 \leftarrow \rightarrow Li_{0.5}VO_2$$

The cyclic voltammogram of the vanadium oxide electrode exhibits five reduction peaks at 3.36, 3.15, 2.89, 2.53 and 2.24 V vs. Li^+/Li (the peak at 3.6 V may appear as a shoulder peak), which are well corresponding to these plateaus (Fig. 4b). The molar ratio between V^{4+} and V^{5+} is calculated as 0.19:1 based on the areas of the discharge peaks on the CV curve. The electrode delivers a specific discharge capacity of 254 mAh g^{-1} in the first cycle, and still maintains 237 mAh g^{-1} after 50 cycles and 200 mAh g^{-1} after 100 cycles (Fig. 4c). Such a cycling performance is better compared to the results reported in the literature where the capacity usually decreases to around 200 mAh g^{-1} after 30–50 cycles [24–26]. As for its rate capability, the specific discharge capacity reaches 215 mAh g^{-1} at 1.8 C, 115 mAh g^{-1} at 18 C and then goes back to above 235 mAh g^{-1} at 0.9 C (Fig. 4d).

For the purpose of addressing the needs of high power applications such as electric vehicles (EV) or hybrid electric vehicles (HEV), high energy efficiency and good rate capability are necessary for the electrode materials of LIBs. Nevertheless, it is partially irreversible for the lithium intercalation/deintercalation between δ-LiV_2O_5 and γ-$Li_2V_2O_5$, resulting in capacity fading when the V_2O_5 electrode is cycled between 2.0 and 4.0 V vs. Li [26,27]. Thus, we narrow down the electrochemical window to 2.5–4.0 V in order to achieve better cycling performance (Fig. 5). In this voltage range, the theoretical capacity from V_2O_5 to LiV_2O_5 is 147 mAh g^{-1}. When the discharge current density is 5 C (1 C = 147 mA g^{-1}), the

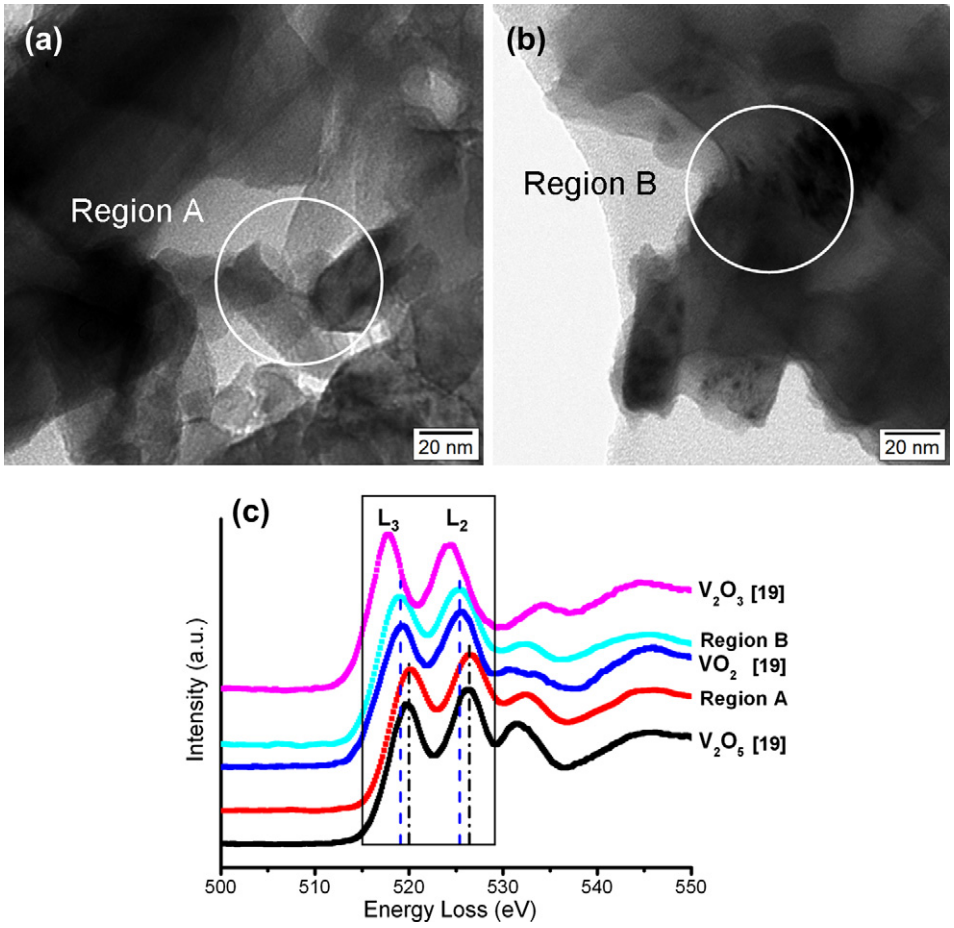

Fig. 3. (a and b) TEM images of the regions for EEL spectrum measurement; (c) corresponding EEL spectra for comparison, the EEL spectra of reference samples (V_2O_5, VO_2 and V_2O_3) are also given [19].

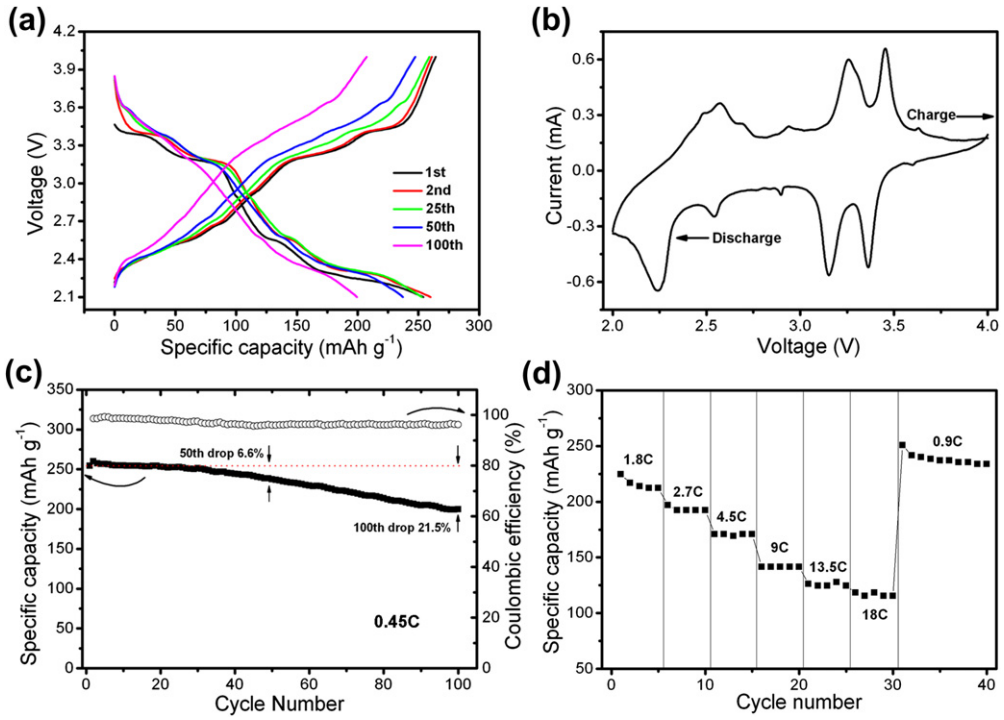

Fig. 4. The electrochemical performances of the vanadium oxide film in the voltage range between 2.1 and 4.0 V: (a) the voltage profile at a cycling rate of 0.45 C; (b) CV curve (third cycle) with the scan rate of 0.2 mV s^{-1}; (c) cycling performance; (d) rate capability at 0.9 C charge rate (1 C = 294 mA g^{-1}).

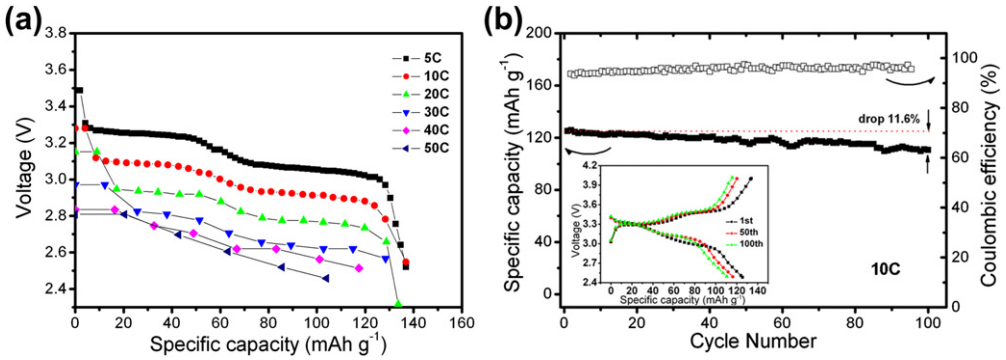

Fig. 5. The electrochemical performances of vanadium oxide film in the voltage range between 2.5 and 4.0 V: (a) the discharge voltage profiles at different discharge rates with a charge rate of 1 C (1 C = 147 mA g^{-1}); (b) cycling performance at 10 C charge/10 C discharge rates and the voltage profiles (inset of b).

electrode can deliver a specific capacity of 137 mAh g^{-1}. With increasing the current density to 50 C, a capacity of 103 mAh g^{-1} is still retained (Fig. 5a). This rate capability is better than that of carbon coated V_2O_5 electrodes [8]. In fact, we have also reported monodisperse V_2O_5 microspheres with capacities of 110 mAh g^{-1} at 9 C and 90 mAh g^{-1} at 15 C in the same voltage range [28]. Moreover, under the conditions of 10 C charge/10 C discharge, this electrode maintains a capacity of 110 mAh g^{-1} (88.4% of the first-cycle capacity) up to 100 cycles (Fig. 5b). It can be seen from the voltage profiles that the voltage plateau does not change too much at the high rate of 10 C until 100 cycles (inset of Fig. 5b).

The rate capability of the film at low temperature conditions is also explored (Fig. 6). The voltage profiles at different discharge rates and at temperatures of −10 °C and −20 °C are shown in Fig. 6a and b. The distance between charge and discharge voltage plateaus increases with decreasing temperature due to the higher polarization. When the cell is cycled at −10 °C, it exhibits a capacity of 107 mAh g^{-1} at 1 C, 41 mAh g^{-1} at 40 C and back to 107 mAh g^{-1} at 1 C again (Fig. 6c). When the temperature is lowered to −20 °C, the cell delivers a capacity of 85 mAh g^{-1} at 1 C, 35 mAh g^{-1} at 10 C and then goes back to 88 mAh g^{-1} at 1 C (Fig. 6d). Our result indicates that this ESD-derived V_2O_5 electrode possesses a low-temperature performance similar to that of the V_2O_5 nanofibers reported by Martin et al. (63.8 and 33.5 mAh g^{-1} at 1 C and 10 C, respectively, at −20 °C) [29].

Fig. 7a shows the CV curves of the vanadium oxide electrode in the third cycle at different temperatures using a scan rate of 0.1 mV s^{-1}, in which the voltage difference (ΔV) between the corresponding anodic and cathodic peaks can be easily measured. This value can be used as a parameter to estimate the polarization level. For example, ΔV values for the peaks associated with the 0.5 lithium ion extraction/intercalation at temperature of 25, 0 and −10 °C are 0.1, 0.16 and 0.3 V, respectively, which indicates that the polarization increases with decreasing temperature.

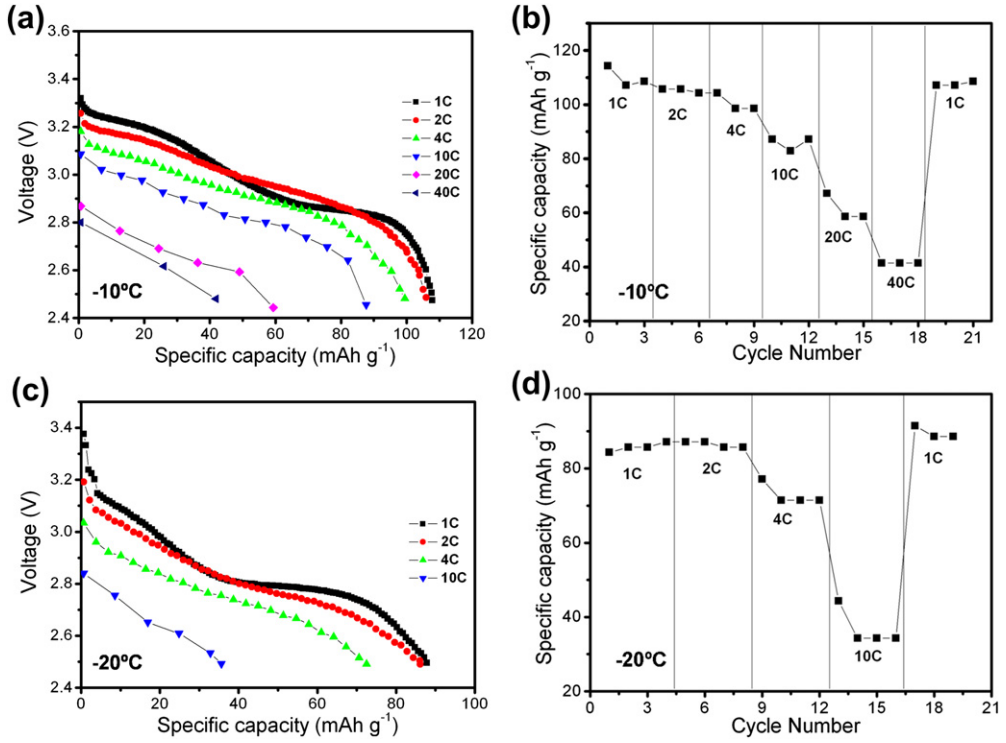

Fig. 6. Low-temperature performance of the vanadium oxide film at −10 °C and −20 °C: the discharge voltage profiles (a and c) and the rate capability (b and d). The charge rate was fixed at 1 C.

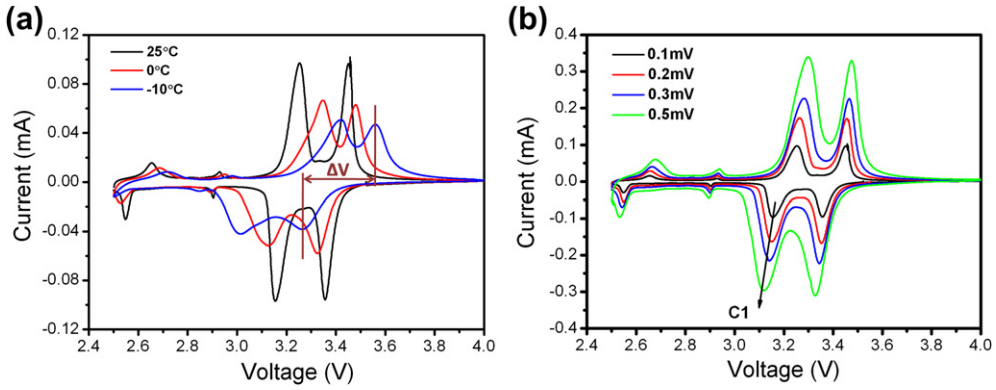

Fig. 7. The CV curves of the vanadium oxide film electrode in the third cycle at various temperatures and a scan rate of 0.1 mV s^{-1} (a) and those measured at 25 °C with different scan rates (b).

In order to investigate the electrode kinetics, the diffusion coefficient of lithium ions in vanadium oxide at various temperatures can be calculated based on the CV curves at the scan rates of 0.1, 0.2, 0.3 and 0.5 mV s^{-1}. The cathodic C1 peaks are marked in Fig. 7b, which correspond to 0.5 lithium intercalation into $Li_{0.5}V_2O_5$ to form LiV_2O_5 at 25 °C. Note that, the CV curves measured at 0 and −10 °C are similar but not shown here. Fig. 8a shows the linear relationship between the peak current (i_p) of C1 peak and the square root of scan rate ($\nu^{1/2}$). If the charge transfer at the interface of the electrode is fast enough and the rate limiting step is the lithium diffusion, there is an equation as following:

$$i_p = \left(2.69 \times 10^5\right) n^{3/2} S D_{Li^+}^{1/2} C_{Li}^* \nu^{1/2}$$

where i_p is the peak current (A), n the charge-transfer number, S the contact area between electrode and electrolyte (here the geometric area of electrode, 0.95 cm^2, is used for simplicity), ν the potential scan rate (V s^{-1}), and C_{Li}^* is the concentration of lithium ions in the cathode (mol cm^{-3}), which is calculated as: $C_{Li}^* = m/(N_A V_{V_2O_5})$. Here, $m = 1$ is the lithium number in the unit cell of LiV_2O_5, N_A is Avogadro's constant (6.022×10^{23}), and $V_{V_2O_5}$ is the volume of unit cell of V_2O_5 ignoring slight volume change during the lithium insertion and extraction processes. Thus, based on the slopes in Fig. 8a, the lithium ion diffusion coefficient D_{Li}^+ is calculated to be 5×10^{-11}, 2.05×10^{-11} and 1.75×10^{-11} cm^2 s^{-1} for 25, 0 and −10 °C. Owing to the high porosity of the film, the D_{Li}^+ value at 25 °C obtained here is higher than the literature results [30–32] although they are still in the same order of magnitude. No data for the temperatures 0 and −10 °C can be found in literature. Fig. 8b displays the relationship between logarithmic D_{Li}^+ and the inverse of temperature. The resultant plots follow the conventional Arrhenius equation:

$$D_{Li^+} = D_0 \exp\left(\frac{-E_a}{RT}\right)$$

where D_0 is the pre-exponential factor (a temperature independent coefficient), E_a the activation energy, R the gas constant, and T the absolute temperature. Thus, the activation energy is calculated as 20.2 kJ mol^{-1}.

The superior performance of this vanadium oxide electrode can be resulted from the following aspects: (1) the porous structure and nanocrystals provide sufficient electron transport pathways and short diffusion distance for lithium ions; (2) the binder-free characteristic is beneficial to the electrical conductivity of electrode. These excellent performances should be very attractive for the large scale and high power applications.

4. Conclusions

A novel vanadium oxide film consisted of walnut-like particles has been fabricated by electrostatic spray deposition. Each particle is composed of lots of nanocrystals (50–80 nm). In the voltage range of 2.1–4.0 V, such a nanoporous vanadium oxide film can deliver a high reversible capacity (above 200 mAh g^{-1}). In the voltage range of 2.5–4.0 V, it shows excellent rate capability (103 mAh g^{-1} at 50 C), stable capacity retention (retaining 110 mAh g^{-1} after 100 cycles at 10 C charge/discharge), good low temperature performance (−10 °C, 41 mAh g^{-1} at 40 C). The

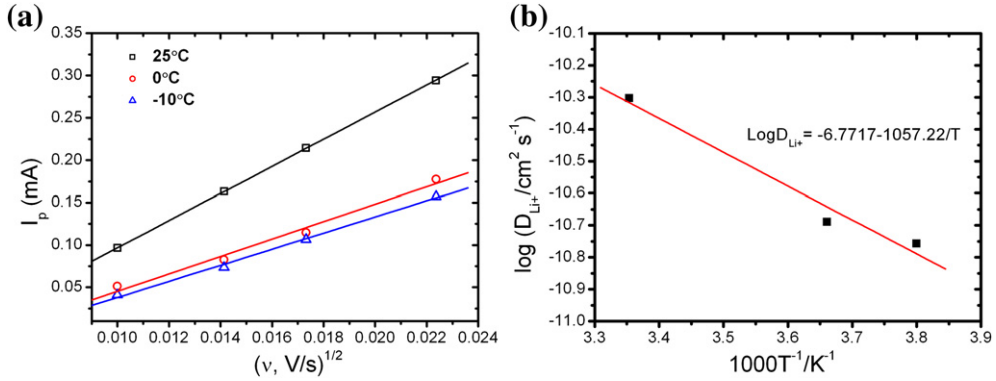

Fig. 8. (a) The relationship between the peak current (i_p) of the cathodic peak C1 and the square root of scan rate ($\nu^{1/2}$); (b) Arrhenius plot of the chemical diffusion coefficient of lithium ions of the electrode.

excellent electrochemical performance is ascribed to its unique nanostructure that improves electrolyte infiltration into particles and facilitates Li-ion diffusion in the electrode. These results indicate that the vanadium oxide film has potential applications as a cathode material in lithium batteries due to its large capacity and high rate capability.

Acknowledgments

This study was supported by National Science Foundation of China (grant nos. 20971117 and 10979049) and Education Department of Anhui Province (grant no. KJ2009A142). We are also grateful to the Solar Energy Operation Plan of Academia Sinica.

References

[1] J.M. Tarascon, M. Armand, Nature 414 (2001) 359.
[2] Y. Wang, K. Takahashi, K. Lee, G.Z. Cao, Adv. Funct. Mater. 16 (2006) 1133.
[3] E.A. Ponzio, T.M. Benedetti, R.M. Torresi, Electrochim. Acta 52 (2007) 4419.
[4] C.O. Dwyer, V. Lavayen, D.A. Tanner, S.B. Newcomb, E. Benavente, G. González, C.M.S. Torres, Adv. Funct. Mater. 19 (2009) 1736.
[5] T. Watanabe, Y. Ikeda, T. Ono, M. Hibino, M. Hosoda, K. Sakai, T. Kudo, Solid State Ionics 151 (2002) 313.
[6] J. Muster, G.T. Kim, V. Krstic, J.G. Park, Y.W. Park, S. Roth, M. Burghard, Adv. Mater. 12 (2000) 420.
[7] C.V.S. Reddy, S.A. Wicker Sr., E.H. Walker Jr., Q.L. Williams, R.R. Kalluru, J. Electrochem. Soc. 155 (2008) A599.
[8] M. Koltypin, V. Pol, A. Gedanken, D. Aurbach, J. Electrochem. Soc. 154 (2007) A605.
[9] V.M. Mohan, B. Hu, W. Qiu, W. Chen, J. Appl. Electrochem 39 (2009) 2001.
[10] J.K. Lee, G.P. Kim, I.K. Song, S.H. Baeck, Electrochem. Commun. 11 (2009) 1571.
[11] J.L. Allen, T.R. Jow, J. Wolfenstine, J. Power Sources 159 (2006) 1340.
[12] J.R. Li, Z.L. Tang, Z.T. Zhang, Electrochem. Solid-state Lett. 8 (2005) A570.
[13] Y. Yu, C.H. Chen, J.L. Shui, S. Xie, Angew. Chem. Int. Ed. 44 (2005) 7085.
[14] Y. Yu, Y. Shi, C.H. Chen, Nanotech 18 (2007) 055706.
[15] L. Wang, L.C. Zhang, I. Lieberwirth, H.W. Xu, C.H. Chen, Electrochem. Commun. 12 (2010) 52.
[16] D. Larcher, G. Sudant, R. Patrice, J.M. Tarascon, Chem. Mater. 15 (2003) 3543.
[17] L.S. Zhong, J.S. Hu, H.P. Liang, A.M. Cao, W.G. Song, L.J. Wan, Adv. Mater. 18 (2006) 2426.
[18] S.L. Jin, H.G. Deng, D.H. Long, X.J. Liu, L. Zhan, X.Y. Liang, W.M. Qiao, L.C. Ling, J. Power Sources 196 (2011) 3887.
[19] N. Ding, X.Y. Feng, S.H. Liu, J. Xu, X. Fang, I. Lieberwirth, C.H. Chen, Electrochem. Commun. 11 (2009) 538.
[20] T. Gallasch, T. Stockhoff, D. Baither, G. Schmitz, J. Power Sources 196 (2011) 428.
[21] M. Broussely, F. Perton, J. Labat, R.J. Staniewicz, A. Romero, J. Power Sources 43 (1993) 209.
[22] C. Delmas, H. Cognac-Auradou, J.M. Cocciantelli, M. Menetrier, J.P. Doumerc, Solid State Ionics 69 (1994) 257.
[23] N.A. Chernova, M. Roppolo, A.C. Dillonb, M.S. Whittingham, J. Mater. Chem. 10 (2009) 2526.
[24] L.Q. Mai, L. Xu, C.H. Han, X. Xu, Y.Z. Luo, S.Y. Zhao, Y.L. Zhao, Nano Lett. 10 (2010) 4750.
[25] A.Q. Pan, J.G. Zhang, Z.M. Nie, G.Z. Cao, B.W. Arey, G.S. Li, S.Q. Liang, J. Liu, J. Mater. Chem. 20 (2010) 9193.
[26] S.H. Ng, T.J. Patey, R. Buechel, F. Krumeich, J.Z. Wang, H.K. Liu, S.E. Pratsinis, Phys. Chem. Chem. Phys. 11 (2009) 3748.
[27] J.M. Cocciantelli, J.P. Doumerc, M. Pouchard, M. Broussely, J. Labat, J. Power Sources 34 (1991) 103.
[28] S.Q. Wang, Z.D. Lu, D. Wang, C.G. Li, C.H. Chen, Y.D. Yin, J. Mater. Chem. 21 (2011) 6365.
[29] C.R. Sides, C.R. Martin, Adv. Mater. 17 (2005) 125.
[30] V. Vivier, J. Farcy, J.P. Pereira-Ramos, Electrochim. Acta 44 (1998) 831.
[31] P. Ragupathy, S. Shivakumara, H.N. Vasan, N. Munichandraiah, J. Phys. Chem. C 112 (2008) 16700.
[32] F. Lantelme, A. Mantoux, H. Groult, D. Lincot, J. Electrochem. Soc. 150 (2003) A1202.